SLAC-PUB-2755
June 1981
(T/E)

LATTICE PREDICTIONS FOR LOW Q^2 PHENOMENOLOGY*

Eve Kovacs†
Stanford Linear Accelerator Center
Stanford University, Stanford, California 94305

ABSTRACT

Recent results of Monte Carlo simulations for SU(3) lattice gauge theories are used to make quantitative predictions which can be compared with QCD phenomenology. In particular, lattice results are used to predict the onset of nonperturbative effects and to determine the interquark potential. The relationship between Λ_0 and the short distance scale of the $q\bar{q}$ potential is also calculated. The predictions are in agreement with theoretical expectations, but indicate that fermions must be incorporated into the lattice calculations before any realistic results relevant to QCD can be derived.

Submitted to Physical Review D

---

* Work supported in part by the Department of Energy under contract DE-AC03-76SF00515, by the University of Melbourne Travelling Scholarship, and by the Lady Leitch Scholarship.

† Address after October 1, 1981: Department of Physics, Rockefeller University, New York, N.Y. 10021.

I. INTRODUCTION

Recently there have been many studies of pure SU(3) lattice gauge theories using Monte Carlo simulations[1] and Hamiltonian[2] and Euclidean[3] strong couplings expansions. In each case the running coupling constant has exhibited a rapid crossover from strong to weak coupling behavior. Assuming that the qualitative features of the results will be unaltered by the inclusion of light fermions, we find from lattice studies, increasing evidence that QCD can simultaneously exhibit the properties of confinement and asymptotic freedom.

In fact, since all of the above calculations yield the same picture, a consistent quantitative description of the behavior of the running coupling constant emerges. For SU(3) lattice gauge theories with the Wilson form of the action[4], the crossover from the perturbative to the nonperturbative regime occurs at a value of $g_0(a) \sim 1$, where g_0 denotes the lattice coupling constant defined in the presence of the lattice cutoff, a. However, since $g(Q^2)$ is a more commonly used variable than $g_0(a)$ it would be useful to know how the lattice results translate into a more conventional momentum space description. The location in Q^2 of the crossover region from weak to strong coupling behavior is of particular interest.

The behavior of Wilson loops on the lattice has also been extensively studied. In continuum QCD the potential between two static color sources separated by a distance R is evaluated from the expectation values of Wilson loops, $\mathrm{Tr}\ P\ \exp\left[ig \oint_C A_\mu^a T^a dx^\mu\right]$, and is given by

$$V(R) = \lim_{T\to\infty}\left[-\frac{1}{T}\,\ell n\left(\mathrm{Tr}\left\langle 0\left|P\left\{\exp\left[ig\oint_C A_\mu^a T^a dx^\mu\right]\right\}\right|0\right\rangle\right)\right] . \qquad (1.1)$$

Here P denotes path ordering, and A_μ^a and T^a denote the color gauge fields and group generators respectively, a being the color index. So, using the expectation values of Wilson loops measured in Monte Carlo simulations and assuming that the continuum limit of the theory is the same as the weak coupling limit, we can obtain a lattice prediction for the interquark potential.

It is important to note that in lattice gauge theories the Wilson loop

$$W(C) = \left\langle \frac{1}{N}\,\mathrm{Tr}\left(\prod_C U\right)_P \right\rangle , \qquad (1.2)$$

where U denotes the usual link operators[5], is defined around a closed contour C comprised of links in the lattice. Consequently only rectangular Wilson loops are considered, which in the continuum limit is equivalent to studying the interaction between two spatially separated static color sources as given in (1.1). We are thus considering a theory which should be equivalent to QCD with infinitely massive quarks.

From the $m_q \to \infty$ limit of the continuum theory we can form some expectations about the behavior of the lattice potential at very short and very long distances. At short distances perturbative calculations should be valid and (1.1) is dominated by single gluon exchange. Hence for SU(3)

$$V(\vec{q}^{\,2}) \sim \frac{-4/3\ \alpha_s(\vec{q}^{\,2})}{\vec{q}^{\,2}} , \qquad (1.3)$$

where $\alpha_s = g^2/4\pi$. The coordinate space version of (1.3) is obtained by a Fourier transform. At long distances, although we cannot calculate explicitly, the success of various phenomenological models such as the potential models for $c\bar{c}$ and $b\bar{b}$ spectra and the results of string models imply a linearly confining potential $V(R) \sim KR$, where K is the string tension.

It has been shown[6] recently that in the continuum string model in the large distance limit, there is an additional contribution to the potential, $(d-2)/24\pi R$, d being the number of spacetime dimensions. This term is a consequence of string dynamics, not asymptotic freedom. Its presence has also been noted in studies[7] of the roughened phase in the Hamiltonian formulation of lattice gauge theories.

The origin of the correction in lattice theories can be understood by observing that at strong coupling an unroughened string of finite width exists between quarks located on principal axes of the lattice. At sufficiently weak coupling it undergoes a phase transition to a roughened string with unbounded transverse fluctuations, which induce inverse power law corrections to the potential as in the continuum model.

The presence of the roughening transition also causes a weak non-analyticity in the string tension K and limits the usefulness of extrapolating strong coupling expansions to the weak coupling limit. Monte Carlo calculations using planar Wilson loops may also be subject to a systematic error, since it is assumed that K survives to the continuum limit. No evidence for any roughening transition is however observed. The issue would be settled by repeating the Monte Carlo calculations for nonplanar Wilson loops.[8]

Unfortunately it is unlikely that the presence of the additional 1/R term will ever be clearly seen in physical systems. Although no phenomenological model has so far been sufficiently sensitive to demonstrate its existence, the relative importance of the term becomes greater at shorter distances within the nonperturbative regime. Inverse scattering reconstructions of the potential[9] indicate, however, that states for heavier $q\bar{q}$ systems lie quite deeply in the potential well where conventional gluon exchange effects are dominant.

It is worth pointing out here that lattice gauge theories are well known to exhibit confinement naturally in the strong coupling limit. Furthermore, the string tension is an undetermined dimensionful parameter which must be chosen in order to set the QCD scale.[10] Hence any calculation of the interquark potential from lattice measurements of the Wilson loop is guaranteed to exhibit the desired behavior at large R. The areas of interest lie in the short distance region where the lattice potential should reproduce the results of continuum theory and also in the cross-over region, which connects the perturbative and nonperturbative domains.

We can compare the lattice prediction with phenomenologically determined potentials, although we do not a priori expect them to agree at short distances due to the absence of light fermions in the lattice analysis.

We must also bear in mind that important corrections to the results due to finite size effects may exist. These arise as a consequence of the discrete nature of the lattice, the finite volume of the lattice and the finite extent of the Wilson loops considered. To date however, the Monte Carlo analyses have indicated that surprisingly reliable numerical

estimates can be extracted from relatively small Wilson loops and small overall lattice size.

A brief outline of the paper is as follows: In Sec. II we discuss the lattice prediction for the onset of nonperturbative effects in momentum space. A detailed prediction for the short distance behavior of the lattice potential is made by using the continuum theory in Sec. III. In Sec. IV we evaluate the interquark potential from the Monte Carlo data. Section V contains a discussion of the results.

II. THE ONSET OF NONPERTURBATIVE EFFECTS

One of the results of recent Monte Carlo simulations[1] is a determination of the dependence of the lattice coupling constant, $g_0(a)$, on a. From this we can estimate $(g_0,a)_{cr}$, the crossover point where nonperturbative effects become important. Our aim is to translate these quantities into momentum space.

The maximum momentum corresponding to a particular lattice spacing, a, is given by

$$Q = \frac{\pi}{a} \quad . \tag{2.1}$$

The Monte Carlo points begin to depart from the expected weak coupling behavior at a value of $a^2K \sim 0.7$. Choosing as usual

$$K = \frac{1}{2\pi\alpha'} \tag{2.2}$$

and setting the Regge slope $\alpha' = 0.9\ \text{GeV}^{-2}$ we find an upper limit for the crossover point corresponding to $Q^2_{cr} = 2.5\ \text{GeV}^2$. The extrapolations of

the predicted strong and weak coupling behavior for the lattice coupling constant cross at $a^2K \sim 1.2$ corresponding to a lower limit of $Q^2_{cr} = 1.6\ \text{GeV}^2$.

Hence lattice calculations predict that nonperturbative effects grow rapidly for values of Q^2 less than $Q^2_{cr} \sim 2\ \text{GeV}^2$. Of course, since light fermions have not been included in the analyses so far, the estimate of this point may change. However, the value of Q^2_{cr} obtained is consistent with the observed rapid onset of scaling in this region of Q^2.

The next problem is to translate the values $g_0(a)$, to the effective coupling, $\bar{g}(Q^2)$. Now the functional dependence of g_0 on $1/a$ is the same as that of $\bar{g}$ on Q:[5]

$$\beta(\bar{g}) = \frac{\partial \bar{g}}{\partial \ln Q} = -\frac{\partial g_0}{\partial \ln a} = \beta(g_0) \quad . \tag{2.3}$$

Defining the function $F(g_0)$ to give the dependence of g_0 on a as observed in Monte Carlo simulations, where

$$\ln a^2 = F(g_0) \quad , \tag{2.4}$$

then we can integrate the renormalization group equations to obtain

$$\ln \frac{Q^2}{\mu^2} = F\left[\bar{g}(\mu^2)\right] - F\left[\bar{g}(Q^2)\right] \quad . \tag{2.5}$$

So if $\bar{g}(\mu^2)$ is known, the value $\bar{g}(Q^2)$ can be evaluated.

From the Monte Carlo data, at least down to $Q^2 = Q^2_{cr}$, the behavior of the running coupling constant is well described by the perturbation expansion to the two loop level. For definiteness, we choose $\bar{g}(Q^2)$ to be defined in the momentum subtraction scheme with Λ_{MOM} chosen in the conventional way to avoid ambiguities.[11] Then we have from (2.5)

$$\bar{g}^2(Q^2) = \frac{1}{\gamma_0 \ln \frac{Q^2}{\Lambda^2_{MOM}} + \frac{\gamma_1}{\gamma_0} \ln \ln \frac{Q^2}{\Lambda^2_{MOM}}} \quad , \qquad (2.6)$$

with

$$\gamma_0 = \frac{11}{3}\left(\frac{N}{16\pi^2}\right) \quad ,$$

$$\gamma_1 = \frac{34}{3}\left(\frac{N}{16\pi^2}\right)^2 \quad , \quad \text{for SU(N)} \quad ,$$

and

$$\Lambda_{MOM} = 83.42\ \Lambda_0 \quad ,$$

$$\Lambda_0 = (5 \pm 1.5) \times 10^{-3} \sqrt{K} \quad , \quad \text{for SU(3)} \quad .$$

A plot of (2.6) is shown in Fig. 1. The dotted line shows only the lowest order estimate of $\bar{g}^2(Q^2)$ for comparison.

If we assume that the evolution of the momentum space coupling constant in the strong coupling regime is approximately given by the evolution of $g_0(a)$, then from (2.5)

$$\frac{Q^2}{Q^2_{cr}} = \frac{\ln\left[3\bar{g}^2\left(Q^2_{cr}\right)\right]}{\ln\left[3\bar{g}^2\left(Q^2\right)\right]} \quad . \qquad (2.7)$$

The strong coupling curve shown in Fig. 1 is given by (2.7) with Q^2_{cr} chosen to be 1.6 GeV^2, the point at which the extrapolations of the weak and strong coupling curves cross in the Monte Carlo simulations.

In the same spirit, the translation of the actual Monte Carlo data points shown in Fig. 1 is obtained by assuming that the points are related by

$$\ell n\left(\frac{a_2^2}{a_1^2}\right) = \ell n\left(\frac{Q_1^2}{Q_2^2}\right) = A\left[\bar{g}^{-2}(Q_2^2) - \bar{g}^{-2}(Q_1^2)\right] , \qquad (2.8)$$

where A is a constant to be determined from the data.

The numerical values for $\bar{g}^{-2}(Q^2)$ obtained in the strong coupling region should not be taken too seriously because of the assumptions involved in deriving them. However, it is worth emphasizing two points. First, the rapid change in behavior of $\bar{g}^{-2}(Q^2)$ occurs at a small value of $\bar{g}^{-2}/4\pi$; and second, the rapid growth in the coupling constant would never be obtained by a perturbative expansion in powers of g. This means that if we believe that lattice gauge theories provide an accurate description of continuum QCD and that the inclusion of light fermions not alter the conclusions drastically, then the application of perturbative analyses for these low values of Q^2 is not justified.

III. THE STATIC $Q\bar{Q}$ POTENTIAL AT SHORT DISTANCES

Incorporating the lowest order behavior of $\alpha_s(\vec{q}^2)$ into (1.3) and taking the Fourier transform we obtain[12]

$$V(R) = \frac{8\pi}{33R\,\ell n\,(\Lambda R)} , \quad \Lambda R << 1 . \qquad (3.1)$$

As a prediction for the short distance behavior of the potential, (3.1) is not very useful. The value of Λ, apart from being a scheme dependent quantity, is ambiguous in lowest order. Clearly to make any sensible prediction for the short distance behavior of the lattice $q\bar{q}$ potential we need to evaluate the perturbative expansion for the potential to the

one loop level, with only static sources present. Furthermore, the expansion parameter should be the coupling constant defined in the presence of the lattice cutoff.

Fortunately the perturbative expansion of the potential including all finite terms in any scheme will suffice because we know how to relate expansions in different schemes to one another.[11] It is imperative however that all finite terms to a given order in g^2 be retained, otherwise the relationship between the Λ parameters is lost.

The energy between two static color sources in the one loop approximation,[13] evaluated using a minimal subtraction scheme[14] (MS) in the Feynman gauge ($\alpha = 1$) is given by

$$V_{MS}(\vec{q}^2) = -\frac{g^2_{MS}(\mu^2)C_2(R)}{\vec{q}^2}\left[1 + \frac{g^2_{MS}(\mu^2)C_2(G)}{16\pi^2}\left(\frac{11}{3}\,\ell n\,\frac{\mu^2}{\vec{q}^2} - \frac{11}{3}\gamma + \frac{31}{9}\right)\right]. \tag{3.2}$$

In (3.2) $g^2_{MS}(\mu^2)$ is the coupling constant defined in the MS scheme[14] and γ is Euler's constant. $C_2(R)$ and $C_2(G)$ are the usual Casimir factors for SU(N).

Now we wish to express (3.2) in terms of $g_0(a)$, the coupling defined in the presence of a lattice cutoff. The relationship between $g_{MOM}(\mu^2)$ and $g_0(a)$, where $g_{MOM}(\mu^2)$ is the coupling constant defined in the momentum subtraction scheme has been evaluated for pure SU(2) and SU(3) gauge theories[15] and is given by

$$g^2_{MOM}(\mu^2) = g^2_0(a)\left[1 + g^2_0(a)\left(\frac{11C_2(G)}{48\pi^2}\,\ell n\,\frac{\pi^2}{a^2\mu^2} + R(N)\right) + O\left(g^4_0\right)\right]. \tag{3.3}$$

R(N) is a known finite number depending on the gauge group SU(N).

The relationship between $g_{MOM}(\mu^2)$ and $g_{MS}(\mu^2)$ is well known and is given by

$$g^2_{MS}(\mu^2) = g^2_{MOM}(\mu^2)\left[1 + A(\alpha,n_f)\frac{g^2_{MOM}(\mu^2)}{4\pi} + O(g^4)\right] \quad . \qquad (3.4)$$

The $A(\alpha,n_f)$ are calculated[14] for various values of the gauge parameter α and the number of quark flavors n_f.

From (3.3) and (3.4) for pure SU(N) gauge theories we have

$$g^2_{MS}(\mu^2) = g^2_0(a)\left[1 + g^2_0(a)\left(\frac{11C_2(G)}{48\pi^2}\,\ell n\,\frac{\pi^2}{a^2\mu^2} + R(N) + \frac{A(1,0)}{4\pi}\right) + O(g^4)\right] . \qquad (3.5)$$

Hence (3.2) becomes

$$V_0(\vec{q}^2) = -\frac{C_2(R)g^2_0(a)}{\vec{q}^2}\left[1 + \frac{g^2_0(a)C_2(G)}{16\pi^2}\left(\frac{11}{3}\,\ell n\,\frac{\pi^2}{a^2\vec{q}^2} - J\right)\right] , \qquad (3.6)$$

where

$$J = \frac{11}{3}\gamma - \frac{31}{9} - \frac{4\pi A(1,0)}{C_2(G)} - \frac{16\pi^2 R(N)}{C_2(G)} \quad .$$

Notice that μ^2 has dropped out of (3.6).

Defining Λ_0 in the usual way so that terms of the form $[\text{const}/\ell n(a\Lambda_0)^2]^2$ are absent we obtain

$$g^2_0(a) = \frac{1}{\gamma_0\,\ell n\left(\frac{1}{a\Lambda_0}\right)^2 + \frac{\gamma_1}{\gamma_0}\,\ell n\,\ell n\left(\frac{1}{a\Lambda_0}\right)^2} \quad . \qquad (3.7)$$

So we can write (3.6) as

$$V_0(\vec{q}^2) = -\frac{C_2(R)}{\vec{q}^2}\left[\frac{C_2(G)}{16\pi^2}\left(\frac{11}{3}\,\ell n\,\frac{\vec{q}^2}{\pi^2\Lambda_0^2} + J\right)\right]^{-1} \quad . \qquad (3.8)$$

If J is now absorbed into the argument of the logarithm we have

$$V_0(\vec{q}^2) = -\frac{C_2(R)}{\vec{q}^2}\left[\frac{11C_2(G)}{48\pi^2}\,\ell n\,\frac{\vec{q}^2}{\Lambda_Q^2}\right]^{-1} \quad , \qquad (3.9)$$

where

$$\Lambda_Q = \pi \exp\left(-\frac{3J}{22}\right)\Lambda_0$$

$$= 31.71\,\Lambda_0 \quad \text{for} \quad SU(2)$$

$$= 46.08\,\Lambda_0 \quad \text{for} \quad SU(3) \quad . \qquad (3.10)$$

Note that (3.9) has the same form as (1.3), but now we know the exact relationship between the Λ_Q characterizing the short distance behavior of the potential and the Λ_0 determined from Monte Carlo simulations.

Since we are interested in the relationship between Λ_0 and the scale characterizing the short distance structure of the $q\bar{q}$ potential, we need to consider the expression for the potential in coordinate space. In order to determine the ratio of the two scales it is sufficient to keep only terms up to $O\left[1/\ell n\,(a\Lambda_0)^2\right]$. We thus take the Fourier transform of (3.6) to obtain an expression for $V_0(R)$ in the short distance limit given by

$$V_0(R) = -\frac{C_2(R)g_0^2(a)}{4\pi R}\left[1 + \gamma_0 g_0^2(a)\left(\ell n\,\frac{\pi^2R^2}{a^2} - \frac{3J}{11} + 2\gamma\right) + \ldots\right] . \qquad (3.11)$$

Inserting the expression (3.7) for $g_0^2(a)$ and absorbing constant terms into the definition of Λ, we find that the short distance behavior of the lattice $q\bar{q}$ potential is given by

$$V_0(R) = \frac{12\pi C_2(R)}{11C_2(G)R \ \ell n \ (\Lambda_P R)^2} \quad , \tag{3.12}$$

where

$$\begin{aligned} \Lambda_P &= 56.47 \ \Lambda_0 \text{ for } SU(2) \ , \ n_f = 0 \ , \\ &= 82.07 \ \Lambda_0 \text{ for } SU(3) \ , \ n_f = 0 \ . \end{aligned} \tag{3.13}$$

Since the relationship between the Λ's in different renormalization schemes in the continuum theory is independent of the rank of the gauge group, the ratio of the factors obtained in (3.13) is just the ratio of the Hasenfratz factors for SU(2) and SU(3).

Provided that our assumptions concerning the nature of the continuum limit are satisfied, (3.13) gives a prediction for the short distance scale dependence of the lattice interquark potential in terms of a known quantity, Λ_0. The determination of Λ_P from the measured values for Wilson loops thus provides a consistency check on the lattice calculations. It is also a test of whether meaningful information can be extracted from relatively small loops, since significant finite size effects would lead to deviations from (3.13).

IV. CALCULATION OF THE $Q\bar{Q}$ POTENTIAL FROM THE NUMERICAL DATA

The Monte Carlo procedure measures the lattice average of a rectangular Wilson loop W(I,J) as a function of the coupling constant, with I and J denoting the side lengths of the loop in fundamental lattice units. The lattice average $\langle W(I,J)\rangle$ is evaluated by first bringing the lattice to equilibrium and then averaging the value of W(I,J) over all possible $I \times J$ configurations on the lattice. Errors quoted are the standard deviations for fluctuations obtained over several iterations after reaching equilibrium.

Let us suppose for the moment that J corresponds to the time direction. Then $\langle W(I,J)\rangle$ is the interaction energy between two static color sources in the fundamental representation separated by a distance of Ia. Converting (1.1) into lattice variables we obtain the potential

$$V(Ia) = \lim_{Ja \to \infty} \left\{ \frac{1}{Ja} \left[- \ell n \langle W(I,J) \rangle \right] \right\} \quad . \qquad (4.1)$$

Unfortunately, Monte Carlo simulations cannot be done for infinitely long loops. In fact since the total lattice size is only 6^4 for SU(3), the dimensions of the loops measured extend only to 3×3. Finite size effects could thus be important and it may be necessary to include terms in (4.1) for finite J, that drop out in the limit $J \to \infty$.

For example, a number of cutoff dependent corrections may be present. In particular, terms involving powers of the cutoff will occur in $\langle W(I,J)\rangle$ due to the sharp corners in the loop. The absolute normalization of the loops is also uncertain and in principle depends on the cutoff. Another important contribution to $\langle W(I,J)\rangle$ is a perimeter dependent term due to the self-energy of the static sources which gives rise to an ultraviolet

divergence as $a \to 0$. The interaction energy thus contains, in addition to the potential we wish to determine, an unknown term that is different for each value of the lattice spacing. The various contributions to $\langle W(I,J) \rangle$ can be represented in the following form:

$$\langle W(I,J) \rangle = N(a) \exp \left\{ -V(Ia) \cdot Ja + \text{Perimeter}(a) + \text{Constants}(a) \right\} \quad . \tag{4.2}$$

Two simple parametrizations corresponding to (4.2) come to mind: (i) $\langle W(I,J) \rangle$ asymmetric in I,J; and (ii) $\langle W(I,J) \rangle$ symmetric in I,J. Consider first the asymmetric case given by

$$- \ell n \langle W(I,J) \rangle = V(Ia) \cdot Ja + P_I(a) \cdot Ia + P_J(a) \cdot Ja + C(a) \; ; \; I \leq J \; , \tag{4.3}$$

where $P_I(a)$, $P_J(a)$ and $C(a)$ are cutoff dependent constants to be determined. The condition $I \leq J$ is imposed with the idea that a rectangular $I \times J$ Wilson loop measured on the lattice approximates (4.1) if J is chosen to be the time direction. If $I > J$ we just interchange the assignment of the space and time directions and write

$$- \ell n \langle W(I,J) \rangle = V(Ja) \cdot Ia + P_J(a) \cdot Ia + P_I(a) \cdot Ja + C(a) \; ; \; I > J \; . \tag{4.4}$$

Since there is nothing to distinguish the time direction for finite size loops, the Monte Carlo data for SU(3) is actually symmetric in I and J. Consequently we can use (4.3) alone to determine V(Ia).

In (4.3) we note that the terms $P_I(a)$ and $C(a)$, which would drop out in the limit $J \to \infty$, can be eliminated, but the term $P_J(a)$ can never be

separated from the potential. Thus the quantity we extract from the Monte Carlo data is given by

$$\left[V(Ia) + P_J(a)\right] \quad . \tag{4.5}$$

The presence of the self-energy contribution $P_J(a)$ in (4.5) means that the potential is determined only up to an unknown a dependent constant so that just those values corresponding to multiples of a particular value of a can be compared.

Using (4.3) and a set of the SU(3) Monte Carlo data for some $g_0(a)$ gives us 6 equations for 5 unknowns, $[V(Ia) + P_J(a)]$, $1 \le I \le 3$, $P_I(a)$ and $C(a)$. The system is overdetermined. The procedure adopted is to use the extra equation to obtain an additional estimate of the value of one of the potentials. Ideally, in the absence of finite size effects and statistical fluctuations, all estimates would yield the same value.

The above analysis also allows us to make an estimate of finite size effects. From (4.3) we see that

$$\left[V(Ia) + P_J(a)\right] = \frac{1}{a}\left\{- \ell n \langle W(I,J+1)\rangle + \ell n \langle W(I,J)\rangle\right\} , \; I \le J \; . \tag{4.6}$$

The perimeter dependent and constant terms have cancelled out. Furthermore, the larger the value of J, the better we expect the estimate (4.6) of V(Ia) to be. For example, we note that for $I,J \le 3$ we must set

$$\left[V(2a) + P_J(a)\right] = \frac{1}{a}\left\{- \ell n \langle W(2,3)\rangle + \ell n \langle W(2,2)\rangle\right\} \quad . \tag{4.7}$$

However $[V(a) + P_J(a)]$ can be chosen to be

$$\frac{1}{a}\left\{- \ell n \langle W(1,3)\rangle + \ell n \langle W(1,2)\rangle\right\} \quad , \tag{4.8}$$

or

$$\frac{1}{a}\left\{-\ell n\langle W(1,2)\rangle + \ell n\langle W(1,1)\rangle\right\} \quad . \qquad (4.9)$$

We expect (4.8) to give a better estimate of V(a) than (4.9). The differences between the values obtained using (4.8) and (4.9) can also, in principle, give an indication of the errors involved in using small sized Wilson loops. Unfortunately, the data available for SU(3) are rather limited and more measurements for larger loops would be useful.

Next we consider the case of W(I,J) symmetric in I,J. This parameterization of $\langle W(I,J)\rangle$, which is motivated by the symmetry of the Monte Carlo data in I and J, is given by

$$-\ell n\langle W(I,J)\rangle = \frac{1}{2}\left\{\left[V(Ia)+P(a)\right]\cdot Ja + \left[V(Ja)+P(a)\right]\cdot Ia + C(a)\right\} \quad . \qquad (4.10)$$

In this case we adopt the philosophy that the lattice results average each of the possible interpretations of the time direction for an $I \times J$ loop. The self-energy term is now distributed between the two potentials. Again, for $I,J \leq 3$ the system is overdetermined, this time with 6 constraints for 4 unknowns. As before, by choosing different subsets of the equations generated by (4.10) to determine our potentials we can make some estimate of finite size effects.

The two possibilities chosen for illustration are:

(a) $\{I,J\} = \{1,2\}$: giving 3 estimates for V(3a).

(b) $\{I,J\} = \{1,3\}$: giving 3 estimates for V(2a).

The Monte Carlo data actually gives values of $\langle W(I,J)\rangle$ corresponding to a particular value of g_0. However, we know how g_0 behaves as a function

of a and hence it is a simple matter to calculate the physical scale. The two sets of SU(3) data analysed here correspond to couplings in the weak coupling regime with $g_0^2 < 1$. Hence the corresponding values of a are given by

$$\begin{aligned} a &= \frac{1}{\Lambda_0} \exp\left(-\frac{1}{2\gamma_0 g_0^2}\right)\left(\gamma_0 g_0^2\right)^{-\gamma_1/2\gamma_0^2} \quad , \\ &\sim 0.2 \text{ fm} \quad \text{for} \quad g_0^2 = 0.9916 \quad , \\ &\sim 0.1 \text{ fm} \quad \text{for} \quad g_0^2 = 0.9018 \quad . \end{aligned} \tag{4.11}$$

The values of a are subject to 30% uncertainty due to the uncertainty in Λ_0.[16]

It turns out that for the two values of coupling considered, the corresponding distance scales differ very nearly by a factor of 2. Hence in this case we can chose one of the $P_J(a)$ such that

$$V(a_1) = V(2a_2) \quad , \quad a_1 = 2a_2 \quad .$$

This now leaves one irrelevant additive constant, which corresponds to choosing a zero in the energy scale.

V. DISCUSSION

The results of the calculations described in Sec. IV using the asymmetric parametrization (4.3) and the symmetric parametrization (4.10) are presented in Figs. 2 and 3, respectively. In Fig. 2 the points labeled "large loops" and "small loops" correspond to choosing V(a) given

by (4.8)' and (4.9) respectively, while in Fig. 3 the points labeled "1×1 - 2×2 loops" and "1×1 - 3×3 loops" correspond to the alternatives (a) and (b) respectively as discussed in Sec. IV. Both figures also include for comparison several phenomenological potentials determined from heavy $q\bar{q}$ bound state spectra.[12,17]

The solid lines shown in each figure are plots of

$$V(R) = \frac{16\pi}{33R\ \ell n\left(\Lambda_P R\right)^2} \quad , \qquad R < 0.2 \text{ fm} \tag{5.1}$$

and

$$V(R) = KR \quad , \qquad R > 0.3 \text{ fm} \quad .$$

These plots exhibit the expected long and short distance behavior of the lattice $q\bar{q}$ potential and are the curves along which the data points should lie in these limits. For both figures the absolute normalization of the data points is fixed so that the values for large distances closely approximate the linearly rising part of (5.1). We see that in both cases the data points give a resonable description of the expected short distance behavior of the $q\bar{q}$ potential as calculated in Sec. III,[18] and the transition from Coulomb-like to confining behavior is evident. Errors in the determination of a are not shown while errors due to the statistical fluctuations in $\langle W(I,J)\rangle$ are small.

The spread in the data points for the lattice potential at a particular value of R gives some estimate of finite size effects. Although these are not negligible, it is reassuring to note that there is reasonable agreement between different estimates of the potential within a particular parameterization of $\langle W(I,J)\rangle$ and also between estimates made from the alternative parametrizations (4.3) and (4.10). This indicates that the results are not very dependent on the detailed method of extraction of V(R). In Fig. 2 the values determined from (4.8) using larger

loops are in marginally better agreement with the predicted curve but clearly more data would be required to see any definite trend. If one uses the symmetric parametrization (4.10) there is no reason to suppose that either of the alternatives (a) or (b) yields a more reliable estimate of the potential, as is evident from the scatter of points in Fig. 3.

The finite volume of the lattice is another important effect which must also be considered. In fact, using a lattice periodic over N_t sites in the time direction is equivalent to studying the theory at a temperature of $T = 1/N_t a$. The finite temperature theory is known to exhibit a deconfining phase transition to a Debye screened Coulomb phase for values of the coupling less than some critical value g_0^*. As the lattice size N_t is increased, the transition is driven to weaker values of g_0^*. Thus, it is important to check that for the lattice size in question we are still in the confined phase for all values of g_0 considered.

In a recent study of finite temperature SU(3) gauge theories,[19] the critical temperature was found to be

$$T^* = \Lambda_{MOM} \pm 15\% \quad . \tag{5.2}$$

Using the known renormalization group behavior, we can estimate for any g_0^* the critical lattice size N_t^* below which we are in the deconfined phase:

$$N_t^* = \frac{1}{T^* a} = \frac{\Lambda_0}{T^*} \exp\left(\frac{2}{\gamma_0 g_0^{*2}}\right)\left(\gamma_0 g_0^{*2}\right)^{\gamma_1/2\gamma_0^2} \quad . \tag{5.3}$$

For the Monte Carlo data we find from (5.3) that

$$N_t^* = 5.4 \pm 0.8 \quad \text{for} \quad g_0^{*2} = 0.9916 \quad , \qquad (5.4a)$$

$$N_t^* = 10.7 \pm 1.6 \quad \text{for} \quad g_0^{*2} = 0.9018 \quad . \qquad (5.4b)$$

Recall that the SU(3) analysis was done on a 6^4 lattice.[1] Hence the Wilson loop data corresponding to (5.4a) is probably within the confining phase, whereas the data corresponding to (5.4b) is in some doubt. However the situation is not clear becasue no evidence for the finite temperature phase transition suggested by (5.4b) is observed in any of the Monte Carlo simulations. One possible explanation may be that the small Wilson loops under consideration are not sensitive to phenomena occurring on the scale of the total lattice size.[20] Furthermore, (5.2) has been determined only for nonsymmetric lattices of sizes up to $N_t = 4$ so that an extrapolation is involved in obtaining the values in (5.4). A determination of the dependence of g_0^* on N_t for spacetime symmetric lattices would be useful.[21] It is also interesting to note that a recent study[22] of SU(2) lattice gauge theories has shown that even if the theory is in the deconfined phase, the Debye screening length is so large that one is effectively measuring the Coulomb potential.

Finally, we note that the lattice calculation is in poor agreement with the phenomenological potentials at short distances. In Sec. III, we found that the scale characterizing the short distance behavior of the lattice potential was $82.07\ \Lambda_0$, or approximately 170 MeV. Phenomenological potentials on the other hand are characterized by a scale equivalent to about 400 MeV.[12] Since the phenomenological potentials are determined in the presence of light quarks which are not included in the calculation described in Sec. III, we might attribute the discrepancy between the two scales to the absence of fermions in the lattice analysis.[16]

We can check the sensitivity of potential models to a change in the short distance scale characterizing the potential by attempting to fit the $c\bar{c}$ and $b\bar{b}$ spectra, using (5.1) to approximate the lattice potential. The results for $c\bar{c}$ states are in reasonable agreement with experiment, but the fit to the $b\bar{b}$ spectrum is poor since, by virtue of their greater mass, these states are much more sensitive to the short distance behavior of the potential. The deviation of the lattice potential from the phenomenological potentials is sufficient to spoil the fit to the heavy $q\bar{q}$ spectra. These results thus indicate the need to include fermions in the lattice analysis before any attempt can be made to calculate a realistic value for the scale that characterizes QCD at short distances.

ACKNOWLEDGEMENTS

The author wishes to thank Michael Creutz for generously supplying the necessary data from his Monte Carlo simulations and also R. Blankenbecler, G. Bodwin, S. Gupta, H. Quinn and M. Weinstein for helpful discussions. I would also like to thank G. Bodwin for reading the manuscript. This work was supported in part by the Department of Energy, contract DE-AC03-76SF00515, by a University of Melbourne Travelling Scholarship and by a Lady Leitch Scholarship.

REFERENCES

1. M. Creutz, Phys. Rev. Lett. 45, 313 (1980); M. Creutz, Bad Honnef Lectures, Preprint BNL-27981 (1980); M. Creutz, Copenhagen Lectures, Preprint BNL-27995 (1980).
2. J. B. Kogut, R. B. Pearson and J. Shigemitsu, Phys. Rev. Lett. 43, 484 (1979); J. B. Kogut, R. B. Pearson and J. Shigemitsu, Phys. Lett. 98B, 63 (1981).
3. G. Münster and P. Weisz, Phys. Lett. 96B, 119 (1980).
4. Other forms of the action may yield numerically different approaches to scaling. See C. B. Lang, C. Rebbi, P. Solomonson and B. S. Skagerstam, Phys. Lett. 101B, 173 (1981).
5. M. Creutz, Phys. Rev. D21, 2308 (1980).
6. M. Lüscher, Nucl. Phys. B180, 317 (1981).
7. R. B. Pearson, Santa Barbara preprint, NSF-ITP-80-47; R. B. Pearson, Santa Barbara preprint, NSF-IPT-80-49; J. B. Kogut, D. K. Sinclair, R. B. Pearson, J. L. Richardson and J. Shigemitsu, Phys. Rev. D23, 2945 (1981).
8. E. Kovacs, work in progress.
9. C. Quigg, H. B. Thacker and J. L. Rosner, Phys. Rev. D21, 234 (1980); C. Quigg and J. L. Rosner, Phys. Rev. D23, 2625 (1981); P. Moxhay, J. L. Rosner and C. Quigg, Phys. Rev. D23, 2638 (1981).
10. Note that the numerical value used for K is determined in the presence of light quarks. Due to screening effects this value is expected to be somewhat smaller than the string tension for pure QCD.

11. W. Celmaster and R. Gonsalves, Phys. Rev. D20, 1420 (1979).

12. J. L. Richardson, Phys. Lett. 82B, 272 (1979).

13. W. Fischler, Nucl. Phys. B129, 157 (1977).

14. Note that in the MS scheme used in Ref. 13, $\ell n 4\pi$ terms are also subtracted. The values calculated for $\Lambda_{MOM}/\Lambda_{MS}$ in Ref. 11 must therefore be divided by $\sqrt{4\pi}$ to obtain the correct ratios for the MS scheme of Ref. 13. In particular, for $\alpha = 1$ and $n_f = 0$, $\Lambda_{MOM}/\Lambda_{MS} = 2.170$.

15. A. Hasenfratz and P. Hasenfratz, Phys. Lett. 93B, 165 (1980); P. Weisz, Phys. Lett. 100B, 331 (1981).

16. There is also a systematic error in Λ_0 arising from using the value of K determined in the presence of light quarks instead of that for pure QCD.

17. E. Eichten, K. Gottfried, T. Kinoshita, K. D. Lane and T. M. Yan, Phys. Rev. D21, 203 (1980); A. Martin, Phys. Lett. 93B, 338 (1980); A. Martin, Phys. Lett. 100B, 511 (1981).

18. For SU(3) the data available in this region are very limited. However, the short distance results for SU(2) are in excellent agreement with the prediction (3.13). See E. Kovacs, manuscript in preparation.

19. K. Kajantie, C. Montonen and E. Pietarinen, University of Helsinki preprint, HU-TFT-81-8.

20. L. D. McLerran and B. Svetitsky, Santa Barbara preprint, NSF-ITP-81-08.

21. E. Kovacs, work in progress.

22. G. Bhanot and C. Rebbi, Nucl. Phys. B180, 469 (1981).

FIGURE CAPTIONS

Fig. 1. The coupling constant as a function of Q^2 obtained from the translation of lattice Monte Carlo results into momentum space. The data points shown are obtained from the Monte Carlo data[1] for the quantity $\chi(I,I)$ versus g_0^2.

Fig. 2. The evaluation of the $q\bar{q}$ potential from lattice measurements of Wilson loops using parametrization (4.3). The calculated points are compared with various phenomenological potentials and with the prediction (5.1) for the $q\bar{q}$ potential in the absence of light quarks. The points labeled "large loops" and "small loops" correspond to choosing V(a) given by (4.8) and (4.9) respectively.

Fig. 3. As for Fig. 2 but using parametrization (4.10) to evaluate the potential. The points labeled "1×1 - 2×2 loops" and "1×1 - 3×3 loops" correspond to alternatives (a) and (b) respectively as discussed in Sec. IV.

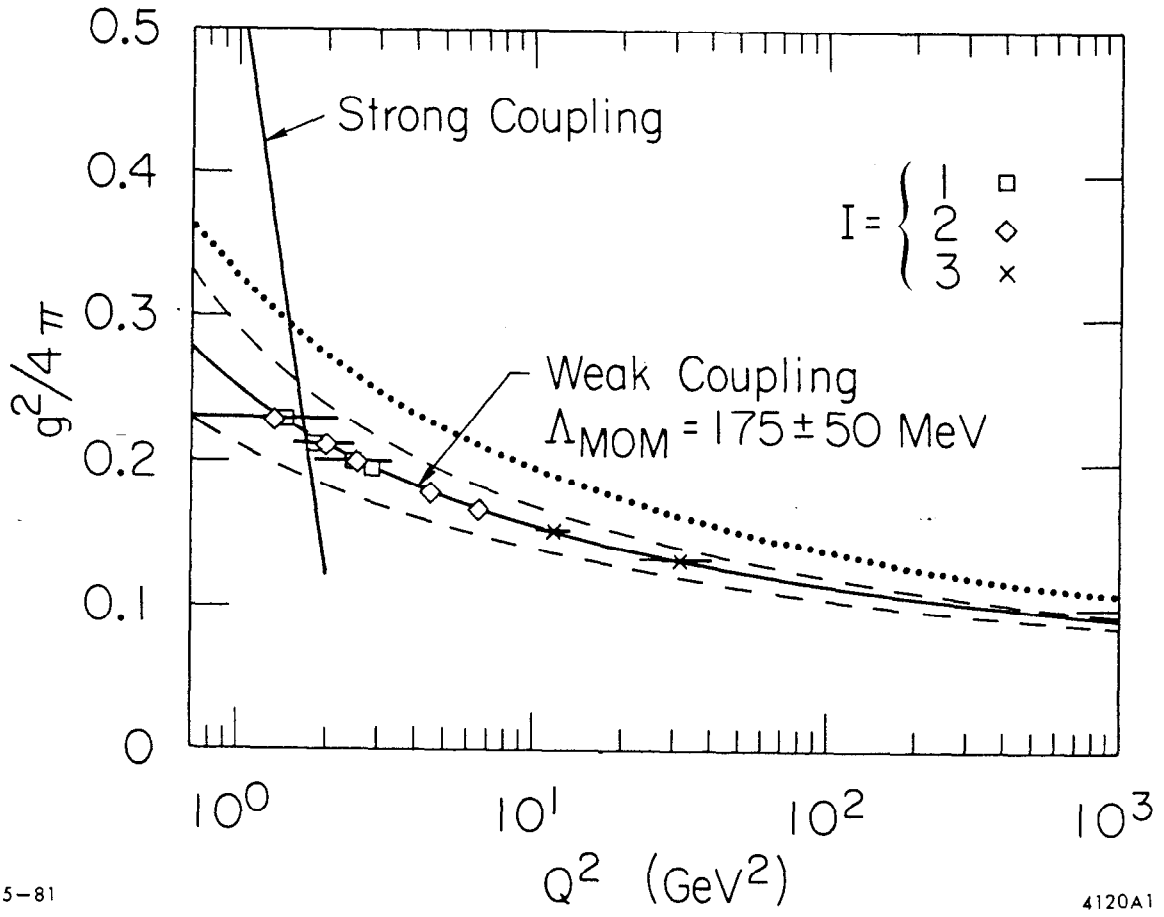
0.5
0.4
0.3
0.2
0.1
0
$g^2/4\pi$
Strong Coupling
Weak Coupling
$\Lambda_{MOM} = 175 \pm 50$ MeV
I = { 1 □ 2 ◇ 3 ×
10^0
10^1
10^2
10^3
Q^2 (GeV^2)
5-81
4120A1

Fig. 1

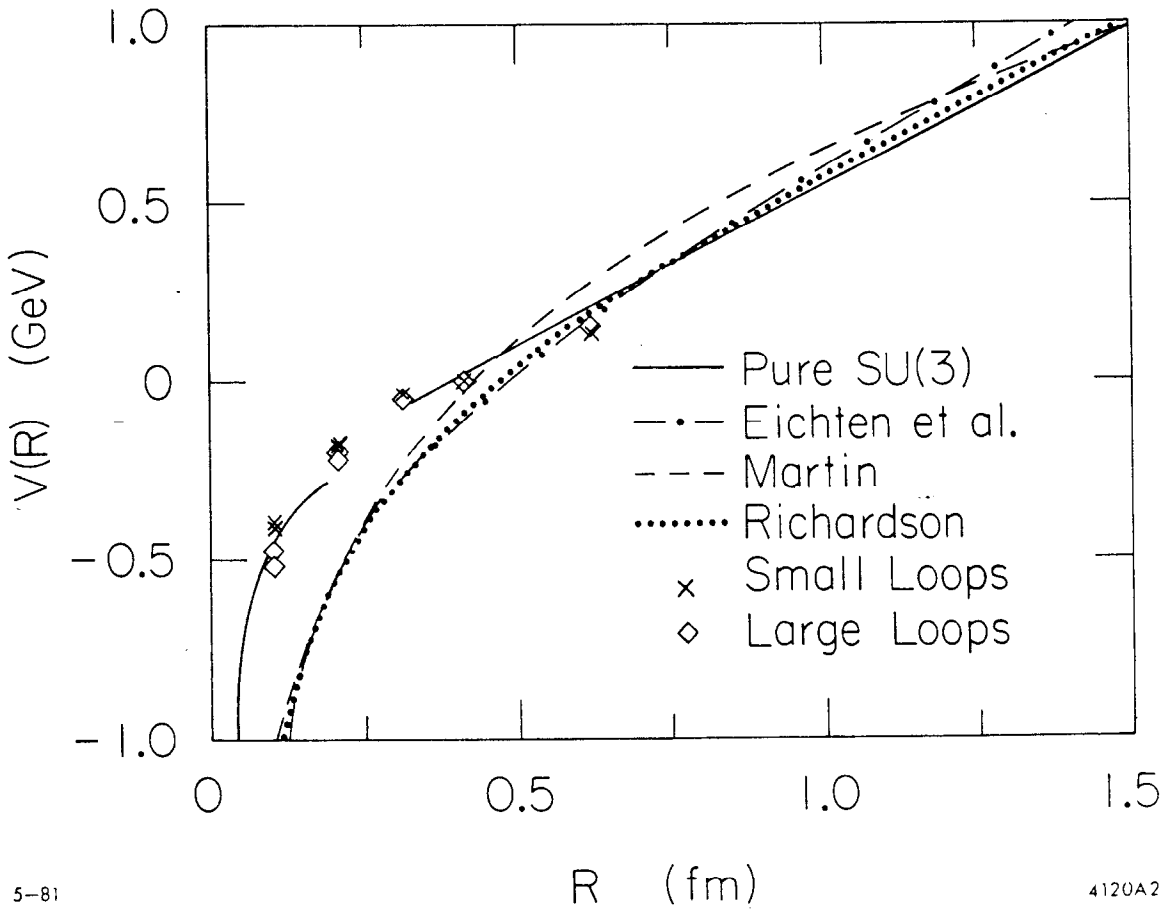
1.0
0.5
0
-0.5
-1.0
V(R) (GeV)
0
0.5
1.0
1.5
R (fm)
Pure SU(3)
Eichten et al.
Martin
Richardson
Small Loops
Large Loops
5-81
4120A2

Fig. 2

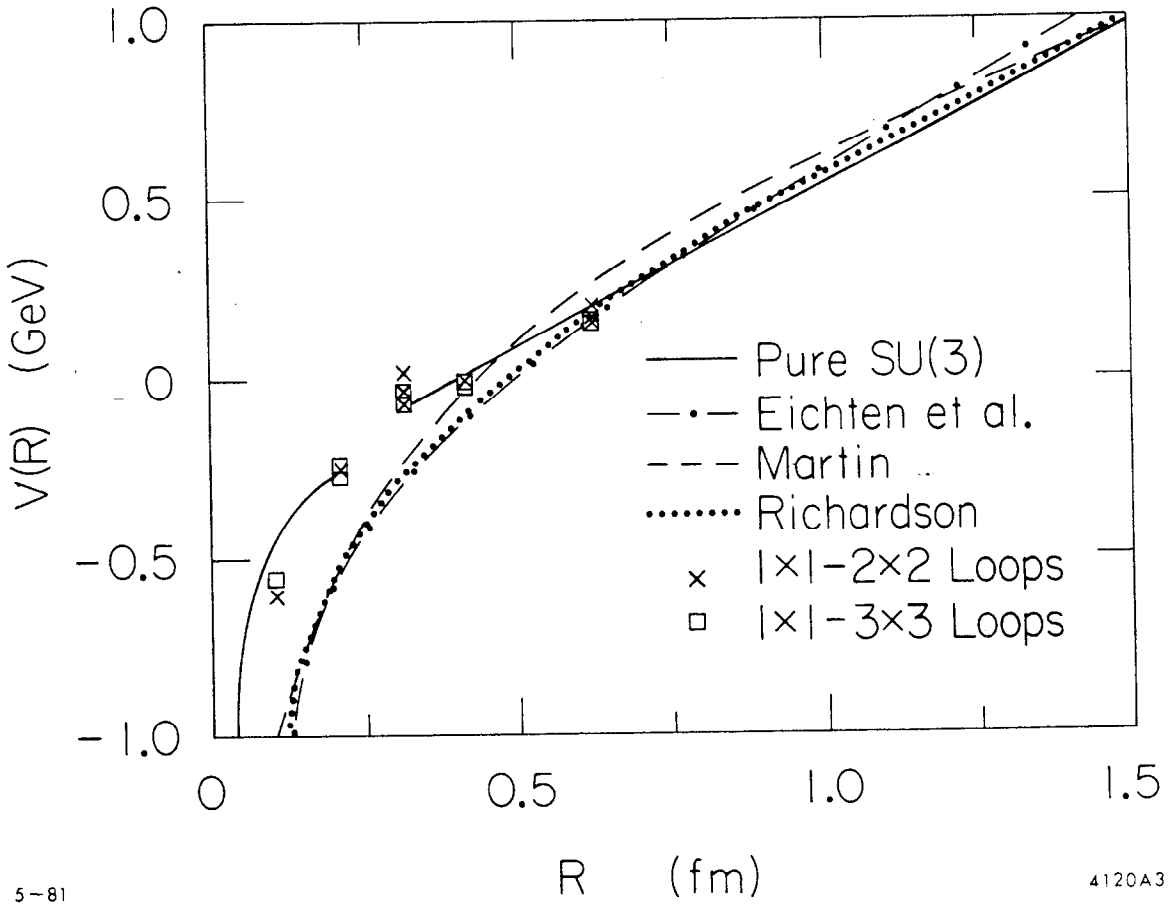
1.0
0.5
0
-0.5
-1.0
V(R) (GeV)
0
0.5
1.0
1.5
R (fm)
Pure SU(3)
Eichten et al.
Martin
Richardson
1×1-2×2 Loops
1×1-3×3 Loops
5-81
4120A3

Fig. 3